

Detection of glutamate in the eye by Raman spectroscopy

Al Katz

City College of New York
Physics Department
Convent Avenue and 137th Street
New York, New York 10031

Erik F. Kruger

New York Eye and Ear Infirmary
Department of Ophthalmology
310 East 14th Street
New York, New York 10003

Glenn Minko

C. H. Liu

City College of New York
Physics Department
Convent Avenue and 137th Street
New York, New York 10031

Richard B. Rosen

New York Eye and Ear Infirmary
Department of Ophthalmology
310 East 14th Street
New York, New York 10003

Robert R. Alfano

City College of New York
Physics Department
Convent Avenue and 137th Street
New York, New York 10031
E-mail: alfano@scisun.sci.cuny.edu

1 Introduction

Glutamate is the principal excitatory neurotransmitter in the central nervous system, including the retina. When released by nerve cells in physiologic quantities, it is involved in a number of normal processes. With nerve cell injury or death from a variety of causes, these cells release their internal stores of glutamate into the surrounding tissue. This overstimulates surrounding nervous cells, initiating a process that results in their demise and the release of even more glutamate. This process has been termed glutamate-mediated neurotoxicity or excitotoxicity. Glutamate-mediated neurotoxicity has been shown to play a role in a variety of ocular diseases including glaucoma, diabetic retinopathy, macular degeneration, and retinal detachment, which together represent a major source of visual disability in the United States. When these disease processes are present, it has been shown that there are increased levels of glutamate in the structurally adjacent vitreous humor, probably due to spillover from glutamate being elaborated by the retina in large quantities. At this time, there are no techniques for the noninvasive measurement of glutamate in the vitreous humor of human eyes. It is only possible to detect the levels of glutamate in the vitreous humor by an invasive technique. This technique measures vitreous humor glutamate levels from eyes undergoing surgery by removing a small amount of vitreous humor and analyzing it by way of conventional biochemical means, such as high performance liquid chromatography. This method clearly suffers

Abstract. Raman spectroscopy is used to detect glutamate in the eye. Glutamate, a by-product of nerve cell death, is an indicator of glaucoma and diabetic retinopathy. The Raman spectra of *ex vivo* whole porcine eyes and individual components (lens, cornea, vitreous) are measured and characterized. Monosodium glutamate is injected into the eyes to simulate disease conditions, and the contribution to the Raman spectrum due to the presence of glutamate is identified. The Raman spectra from the native eye is dominated by vibrational modes from proteins in the lens. An optical system is designed to optimize collection of signal from the vitreous, where the glutamate is located, and reduce the Raman from the lens. Two vibrational fingerprints of monosodium glutamate are detected at 1369 and 1422 cm^{-1} , although the concentrations are much above physiological concentrations. © 2003 Society of Photo-Optical Instrumentation Engineers.
[DOI: 10.1117/1.1559726]

Keywords: Raman spectroscopy; glaucoma; diabetic retinopathy; glutamate.

JBO 02009 received Feb. 22, 2002; revised manuscript received Sep. 23, 2002; and Sep. 30, 2002; accepted for publication Oct. 2, 2002.

from the absence of any value for use in connection with diagnosing and monitoring nonsurgical patients (the majority) over an extended period of time. The development of new, minimally or noninvasive methods, to measure the concentration of glutamate in the vitreous, can serve as both a screening tool and a mechanism for monitoring disease progression and will provide clinicians with valuable information.

The Raman spectra were acquired in *ex vivo* whole and dissected porcine eyes. Monosodium glutamate (MSG) was injected into the eyes to simulate disease conditions, and the Raman spectra with and without MSG were analyzed and compared to determine those Raman bands that provided the highest potential to accurately detected MSG levels in the vitreous. An optical geometry was developed with allowed preferential acquisition of spectra from different regions of the eye. Using this geometry, it was shown that the presence of glutamate in the vitreous could be detected noninvasively in the Raman spectrum.

The eye consists of multiple structures with distinct compositions. Since many of these structures are transparent in the visible and near infrared, potentially they can all contribute their respective signal to Raman measurements performed on the eye. When the excitation light enters the eye through the pupil and signal is collected in a backscattered geometry, as would be employed in a clinical examination, Raman is gen-

erated in the cornea, lens, vitreous, and retina at different levels of intensity. Raman was observed from the cornea, lens, and vitreous. The cornea consist primarily of water and proteins, the major protein component being collagen. The composition of the eye lens is about 65% water and 35% crystallin proteins. The vitreous is composed of 99% water with collagen fibers and hyaluronic acid. It was expected that the Raman contribution from the vitreous would consist primarily of water vibration bands, while the Raman from the lens and cornea would be dominated by amide and C-H modes from the constituent proteins.

The Raman spectra from the different components of the eye have been studied extensively. Preliminary Raman measurements on the eye were reported by the authors.¹ Callender et al.^{2,3} investigated the primary events in vision using resonant Raman scattering. Yu, Kuck, and Askren⁴ measured and characterized the Raman spectrum from the intact rabbit lens. Mizuno et al. directly measured the Raman spectra from intact rabbit and rat lenses,⁵ and used near infrared Fourier transform spectroscopy to measure the Raman spectrum from rabbit cornea and sclera.⁶ Sebag et al.⁷ employed Raman spectroscopy to investigate changes in the vitreous introduced by diabetes. In that work, differences in the Raman relative intensity at two peaks (1604 and 3057 cm^{-1}) was observed between surgical vitreous specimens from patients with proliferative diabetic retinopathy and controls. Yaroslavsky et al.⁸ studied the elastic and Raman scattering properties of the human lens. Borchman et al.⁹ used Fourier transform Raman spectroscopy to study the lipid membranes of *ex vivo* human lenses. Bernstein et al.¹⁰ used resonance-enhanced Raman scattering to study macular carotenoid pigments *in vivo*. Ermakov, McClane, and Gellermann¹¹ measured the concentration of macular carotenoid pigments in the human eye using resonance-enhanced Raman spectroscopy. Although the Raman spectra from the eye and eye components have been studied extensively, there are still numerous obstacles that need to be overcome to successfully detect disease in the eye by implementing a Raman-based monitoring system to measure concentrations of glutamate or other molecules. Some of these include the following. 1. A relatively large near-infrared fluorescence emission from a variety of tissue fluorophores add a background signal that can obscure weaker Raman signals and interfere with quantitative measurements. The fluorescence wing has been reported in the literature,^{12,13} but its origin is not well established. The intensity of this wing decreases at longer wavelengths. 2. The presence of strong Raman signals from proteins in the lens and cornea can obscure the glutamate signature. 3. Risk of retinal damage limits the power of the excitation laser and integration times. Excitation at infrared wavelengths reduces the intensity of the background fluorescence wing and simultaneously reduces risk of damage, thus allowing higher excitation intensity and/or longer integration times.

2 Experimental Method and Results

The Raman spectra from *ex vivo* porcine eyes with and without glutamate was measured to identify the Raman signatures that could serve as markers for the presence of glutamate. Disease conditions were simulated by injecting monosodium glutamate (MSG) into the vitreous of the eyes. The presence

of MSG was identified in the Raman spectra. A strong native Raman signal from the eye limited the effectiveness of these measurements. To overcome this problem, the eyes were dissected and Raman measurements were performed on the individual components of the eye. The contributions to the Raman signal from the different components of the eye were identified, and it was determined that the lens and cornea were the major contributors to the background Raman signal, while the vitreous contribution consisted mostly of the fluorescence wing and Raman from water bands. Based on this knowledge, a modified optical system was designed to reduce collection of Raman signals from the lens and cornea while maintaining efficient collection of Raman signals generated by the glutamate in the vitreous. With this system, we were able to detect the presence of Raman from MSG in the eye.

2.1 Optical System

In the initial series of Raman measurements, the eye specimens were excited either at 632.8 or 800 nm. The excitation power of the helium neon laser is 5 mW. The 800-nm laser is an AlGaAs:GaAs diode laser from Power Technologies (Model HPM900-800-100). The output power measured at the specimen site is 30 mW. With both lasers, the beam was weakly focused inside the specimen. The laser beam entered the eye at the middle of the pupil, and the beam direction was approximately parallel to the optic axis of the eye. A moveable mirror allowed switching the excitation laser without altering the collection geometry. A Nikon camera lens collected the backscattered Raman signal and focused it onto the entrance of a computer-controlled flat field spectrometer (Acton Research Corporation, model Spectra Pro 275). Care was taken to prevent back reflections from being incident on the spectrometer slit. The output of the spectrometer was coupled to a cooled CCD (Princeton Instruments model TEA/CCD 512). The CCD is a 512×512 pixel array. The CCD signal was integrated along the vertical axis (parallel to the slit) prior to digitizing. The resolution of this system is 4 cm^{-1} . Scattered laser light was blocked by a holographic notch filter (Kaiser Optical Systems) positioned at the spectrometer slit. Integration times are computer controlled. For the data presented below, a 60-s integration time was used. Data was digitized with 16-bit resolution and transferred to a personal computer for storage and additional processing.

2.1.1 Optical system for removal of background Raman signal

To eliminate strong background Raman signals from native proteins in the eye, an optical system was designed that could significantly reduce signal from the lens and cornea without significant loss of signal from the vitreous, allowing detection of MSG in the eye. In this optical system, the exciting laser beam is brought to a tight focus inside the vitreous, while maintaining a large beam diameter at the lens and retina. The larger spot size on the retina reduces the risk of laser-induced retinal damage. A description of this system is as follows. In the healthy, living eye, the lens changes focal length with object distance to create a focused image on the retina. However, in a dilated or *ex vivo* eye, the lens images objects at infinity, i.e., the combined focal length of the lens and cornea is equal to the distance from lens to retina. For this situation,

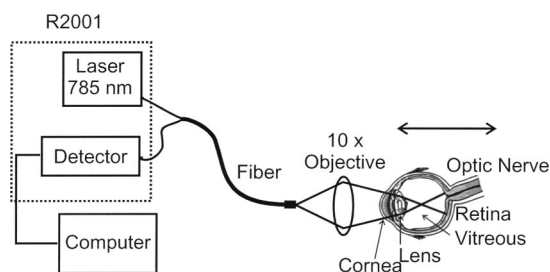


Fig. 1 Schematic of optical system isolating the Raman signal from the vitreous.

a collimated laser beam incident on the lens is brought to a focus on the retina. In the optical system used in this research, the exciting laser beam is first expanded prior to entering the eye, and then brought to a tight focus at a distance of about 2 to 3 cm from the focusing lens. The eye is positioned such that the beam diameter fills the (dilated) pupil and comes to a tight focus in the vitreous, and then expands in diameter at the retina. An aperture in the optics limits signal collection to the region (vitreous) near the focus.

A diagram of the system is shown in Fig. 1. This system is based on the R2001 Raman Spectrometer from Ocean Optics, with additional optics to modify the collection geometry. The exciting diode laser, spectrometer, and CCD detector are integrated components of the R2001. The eye specimens are excited by the diode laser at 785 nm, coupled into a 90- μm optical fiber. The excitation power, measured at the sample site, was 100 mW. A 200- μm collection fiber is mounted in the same jacket as the excitation fiber and serves as the collection aperture. A dichroic mirror/beamsplitter combination is used to make the excitation and collection optics collinear. A notch filter at the tip of the excitation fiber eliminates fluorescence from the laser diode, and fluorescence and Raman generated in the optical fiber. The output beam from the excitation fiber is allowed to expand to a diameter slightly greater than that of the pupil aperture, and is then brought to a tight focus by a 10 \times microscope objective. The distance from the fiber tip to the microscope objective is adjustable.

The signal is detected by a cooled CCD, digitized with a 12-bit analog-to-digital converter, and transferred to a personal computer for storage and processing. The spectral resolution of this system is 30 cm^{-1} . Integration times are computer controlled and can be varied from 50 ms to 240 s. For the data presented next, integration times were typically 60 s.

In this experimental setup, the eye is positioned such that the pupil aperture closely matches the beam diameter as it enters the pupil. The eye lens and cornea provide additional focusing power, which brings the beam to a focus inside the vitreous. The microscope objective also functioned as the collection lens. The small depth of field of this system permitted only signals generated near the focus of the excitation beam to be efficiently coupled into the collection fiber. The distance of the focal point from the retina can be varied by moving the eye relative to the objective. When the eye was positioned closer to the focusing lens, i.e., focusing closer to the retina, the excitation beam came to a focus in the middle of the vitreous, with a large beam diameter at both the eye lens and the retina. In this position, only signals generated in the vit-

reous will be collected by the fiber. Moving the eye forward, i.e., focusing closer to the lens, will result in an increase in Raman signal being detected from the lens and cornea.

2.1.2 Safety issues and power levels

The American Conference of Governmental and Industrial Hygienists (ACGIH) provides a threshold limit value (TLV) for ocular exposure to NIR laser radiation.¹⁴ For an exposure time t , ($1.8 \times 10^{-5} \leq t \leq 10^3$) and for wavelengths in the range of 700 to 1049 nm, the TLV is given by:

$$\text{TLV} = 1.8 C_A t^{3/4} \text{ mJ/cm}^2, \quad (1)$$

where C_A is given by:

$$C_A = 10^{0.002(\lambda - 700)} \quad (700 \leq \lambda \leq 1400 \text{ nm}). \quad (2)$$

For a 1- cm^2 beam spot size on the retina, the TLV at 785 nm is 57 mJ/cm^2 , and therefore the maximum allowed laser power for 60 s exposure is 0.96 mW. Implementation in a clinical setting would require a significant reduction in laser power. Decreasing the laser power will also result in a lower background Raman signal and fluorescence wing emission.

2.2 Specimen Preparation

Raman measurements were performed on *ex vivo* porcine eyes acquired from a local abattoir. The eyes were stored at 4 $^\circ\text{C}$ prior to acquisition of spectra and were typically one to two days old at time of measurement. Eyes for which the cornea was cloudy were rejected, but no other selection process was applied to the eyes.

Disease conditions were simulated by injecting an aqueous solution of MSG into the eyes. The MSG was injected by syringe near the back of the eye to reduce risk of the needle damaging the lens or cornea. The MSG injection added additional fluid, causing the eye to bulge at the lens. This distortion changed the collection efficiency of the Raman system and subsequently the strength of the signal. To reduce this distortion, fluid had to be removed from the eye to restore it back to its approximate original shape.

It was difficult to determine the precise concentration of MSG injected into the vitreous; 2 to 3 ml of a supersaturated aqueous solution of MSG were injected into each eye. The MSG was not uniformly distributed in the vitreous, and it was observed that the Raman signal from the MSG reached a maximum about 5 to 15 min after injection indicating that it took some time for the MSG to diffuse from the point of injection to the laser beam path. A rough estimate is that the amount of MSG injected into the eyes was 100 to 500 mg. For comparison, Dreyer et al.¹⁵ reported glutamate levels of 11 $\mu\text{g/ml}$ in a healthy eye and 27 $\mu\text{g/ml}$ for glaucoma patients.

2.3 Raman Spectra from Glutamic Acid

To identify the positions of the higher intensity Raman emission bands from MSG ($\text{C}_5\text{H}_8\text{NO}_4\text{Na}$), the Raman spectra of MSG powder and aqueous solution were measured and are shown in Figs. 2(a) and 2(b), respectively. The higher intensity Raman bands from the MSG powder had peak emission at 938 and 1416 cm^{-1} . Other, less intense Raman bands were observed at 779, 838, 986, 1032, 1126, 1321, 1508, and 1582 cm^{-1} . In solution, the more intense Raman bands from the

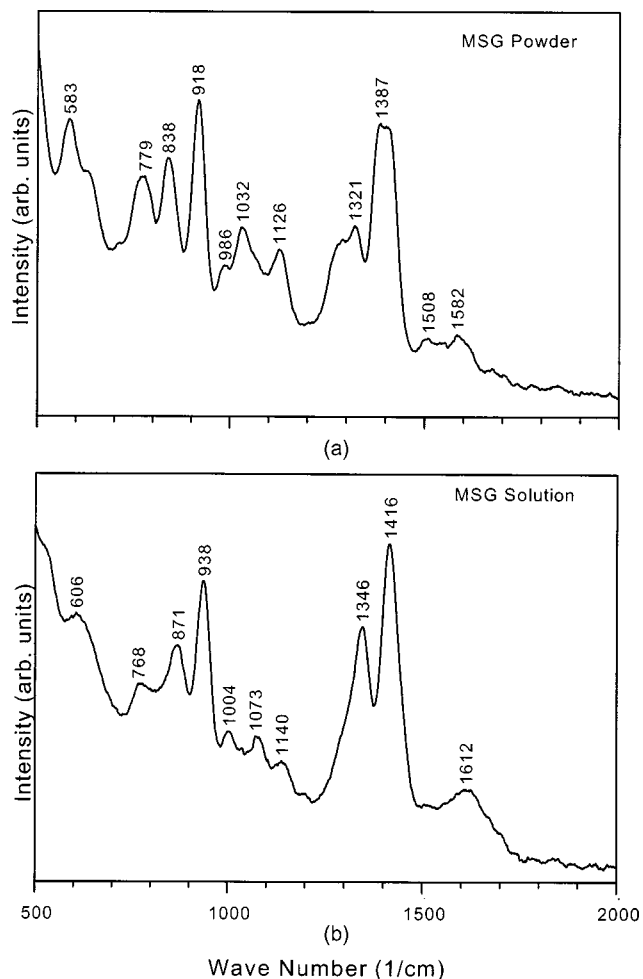


Fig. 2 Raman spectra from MSG: (a) powder and (b) aqueous solution.

MSG were observed at 938, 1346, and 1416 cm^{-1} . Additional Raman bands were observed at 768, 871, 1004, 1073, and 1140 cm^{-1} . The broad emission band seen in Fig. 2(b) at 1612 cm^{-1} is a water band.

2.4 Raman Spectra from Porcine Whole Eyes

Initially the Raman spectra were acquired with 632.8-nm excitation. The helium neon laser was weakly focused in the middle of the vitreous. Some of the major features observed in the spectrum were: the aliphatic and aromatic C-H stretching bands from various proteins at 2930 and 3056 cm^{-1} , respectively; an O-H stretching mode at 2900 cm^{-1} is observed as a shoulder on the low energy side of the more intense 2930 cm^{-1} band; broad bands from water in the 3200 to 3500 cm^{-1} region; and a relatively large fluorescence wing. In the fingerprint region, additional Raman bands were observed in the measured spectra. Most evident were the CH_2 stretching mode at 1445 cm^{-1} and the amide I mode at 1650 cm^{-1} . Weaker bands can be observed at 1233, 1326, and 1533 cm^{-1} . However, the intensity from these Raman bands was significantly weaker than the fluorescence wing.

To reduce the fluorescence wing, the excitation source was changed to a 800-nm diode laser. An additional benefit from the use of an 800-nm excitation source in a clinical setting

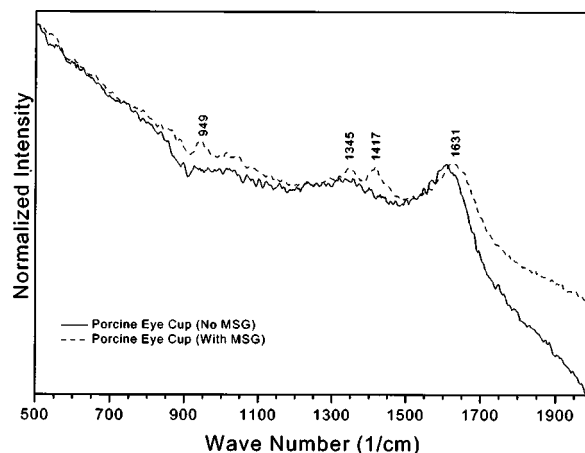


Fig. 3 Raman spectra from porcine eye excited at 800 nm.

would be a reduced risk of retinal damage. The spectra from a typical eye, before and after MSG injection, are shown in Fig. 3. To facilitate comparison between the spectra, the data was normalized to the amide I bands at 1637 cm^{-1} . This band was used for normalization because of the relatively strong native eye signal and the absence of an MSG signal at this wavelength.

Numerous bands were observed in the Raman spectrum from the native eye. Some of the more intense bands were observed at 758, 852, 882, 1003, 1032, 1125, 1237, 1320, 1445, 1538, 1603, and 1658 cm^{-1} . Assignments of many of these bands are in the literature and are repeated here. The 758 and 881- cm^{-1} bands have been assigned to tryptophan.^{4,5,15} The 852- cm^{-1} Raman band is from tyrosine.^{5,15} The 1003 and 1031- cm^{-1} bands have been assigned to phenylalanine.^{4,6,16} The 1237 and 1320- cm^{-1} bands are amide III bands. The 1445- cm^{-1} band is a CH_2 deformation mode. The 1604- cm^{-1} band is from collagen. The 1658- cm^{-1} band is an amide I mode.

MSG was injected into the eyes, and after a five minute delay, the Raman spectra were acquired. The delay allowed time for the MSG to diffuse through the vitreous. Examination of spectra shown in Fig. 3 reveals that after injection of MSG, there is an increase in signal in the region from 900 to 1050 cm^{-1} , with an additional Raman peak appearing at 966 cm^{-1} . The 1346 and 1416- cm^{-1} bands observed in the spectrum from the MSG solution (see Fig. 2) were not observed in the eye spectra. Although the 966- cm^{-1} band was only observed in the eye after MSG injection, it is not clear whether this band is the 938- cm^{-1} band observed in the spectrum of the MSG solution or the 961- cm^{-1} observed in the cornea spectrum (see next). If the 966- cm^{-1} Raman band was from the MSG, then the reason for the shift in peak position is not known. It may be due to differences in the local environment. In either case, the closeness of this band to the strong phenylalanine Raman band at 1003 cm^{-1} and the large background wing may make this band unreliable as a marker for glutamate concentrations in the vitreous.

2.5 Raman Spectra from Porcine Eye Components

The Raman signals from the different eye components were measured to separate the contributions from the different eye

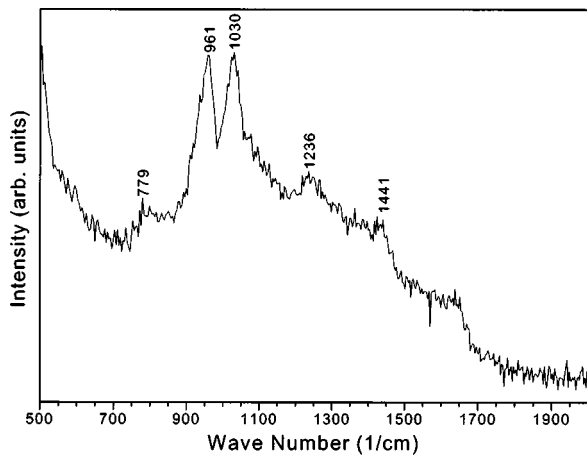


Fig. 4 Raman spectrum from porcine cornea.

components. The cornea and lens were separately removed from the porcine eyes. A typical Raman spectrum from the porcine cornea is shown in Fig. 4. The intensity of the Raman signal and the fluorescence wing from the cornea was an order of magnitude weaker in intensity than from the whole eyes under similar conditions of excitation. Much of the structure observed by Mizuno et al.⁶ in the rabbit cornea was not observed in the porcine specimens. The two strongest Raman peaks were at 961 and 1030 cm^{-1} . Although collagen represents a significant component in the cornea, a Raman spectra distinct to collagen was not evident in these spectra. The amide I and III bands and the CH_2 deformation band signals were observed to be very weak. The short optical path length of the excitation light through the cornea was a contributing factor in the weak corneal signals.

On the other hand, the Raman spectrum from the isolated lens was relatively strong and exhibited considerable structure. The intensity of the fluorescence wing was greatly reduced, thereby improving the signal-to-noise compared to the whole eye spectrum and revealing additional Raman structure in the spectrum. Figure 5 shows a typical Raman spectrum from the porcine lens. The more intense Raman bands were observed at 824, 1004, 1246, 1329, 1447, and 1661 cm^{-1} . Additional Raman bands were observed at 614, 764, 888, 1123, 1329, 1547, 1602, and 1728 cm^{-1} . A comparison of Raman shifts observed in the whole eye to those observed in the lens and cornea indicate that the major contribution to the whole eye Raman spectra is from the lens and cornea.

2.6 Raman Spectra from Eye Cup

To determine if the Raman signature of MSG in the vitreous could be detected, assuming that the cornea and lens signals could be eliminated, Raman spectra were acquired from the eye cup, an eye with the lens and cornea removed. The eye cup Raman spectrum is dominated by contributions from the vitreous. The Raman spectra of the eye cup before and after injection of MSG are shown in Fig. 6. The eye cup spectrum consisted of a large fluorescence wing and the water vibration band near 1630 cm^{-1} . This is to be expected, since the vitreous is 99% water. After injection of MSG, three Raman bands appeared in the eye cup spectrum, located at 949, 1346, and 1417 cm^{-1} . A comparison of this spectrum with the Raman

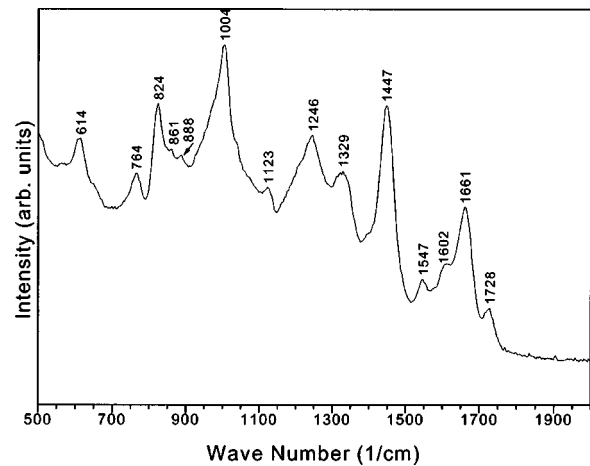


Fig. 5 Raman spectrum from porcine lens.

spectrum of MSG solution [see Fig. 2(b)] reveals that these three bands are very close to the positions of the three strongest Raman bands from the MSG. These measurements provided the evidence that an MSG signature could be detected vitreous, assuming that the background signals from the lens and cornea can be eliminated.

2.7 Raman Spectra Acquired with Confocal Geometry

As before, Raman spectra were acquired from *ex vivo* porcine whole eyes with MSG injected. A typical whole eye spectrum with MSG injected is shown in Fig. 7. This spectrum was acquired with the exciting laser focused near the middle of the vitreous. Significant in the spectrum is the lack of a strong Raman signal from the lens and the presence of two Raman bands at 1369 and 1422 cm^{-1} . These two bands were not present in the native (no MSG injected) eye spectrum and are close to the 1346 and 1416- cm^{-1} bands observed in both the MSG solution (see Fig. 2) and the MSG injected eye cup spectra (see Fig. 6). Therefore it is concluded that these two

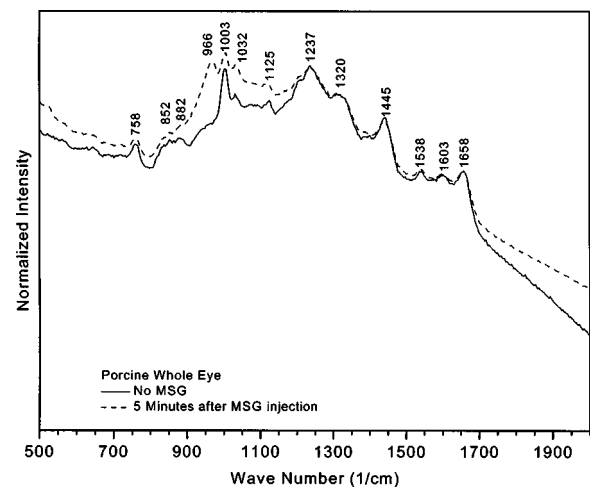


Fig. 6 Raman spectra from porcine eye cup before and after injection of MSG. Spectra were taken from an untreated eye and 5 min after MSG was injected into the eye.

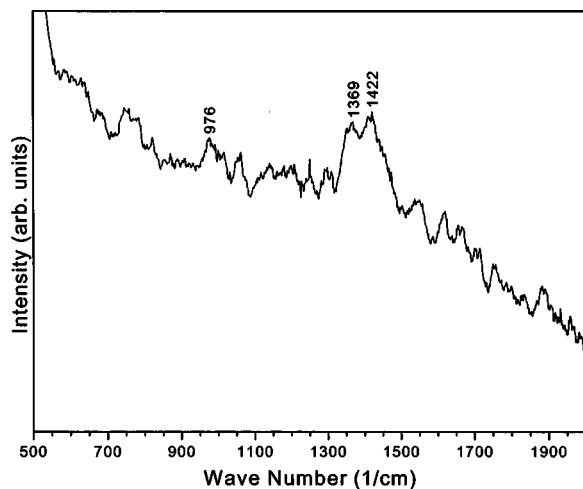


Fig. 7 Raman spectrum from porcine whole eye with MSG injected. Raman signals from the lens and cornea were removed by the optical system.

Raman bands are from the MSG. The 949-cm^{-1} band observed in the MSG injected eye cup spectrum and the 966-cm^{-1} band initially observed in the whole eye (see Fig. 3) were not evident in this spectrum, but a weak band at 976 cm^{-1} , which was not observed in the native eye spectrum, was evident in this spectrum. It is not known if this band is a Raman signal from the MSG.

3 Conclusion

In conclusion, this work has demonstrated that with the proper optical system, it may be possible to use Raman spectroscopy to detect high concentrations of glutamate in the vitreous with minimal background interference from the Raman of the lens and cornea. This research demonstrates the potential to use Raman spectroscopy for real-time, noninvasive measurements of glutamate concentrations in the eye as a marker for macular generation, although the concentrations were much higher than physiological concentrations. Future efforts will concentrate on developing methods to accurately quantify glutamate concentrations and to determine minimum sensitivity levels. Extending this work to a clinical setting would require development of a significantly more sensitive detection system.

Acknowledgment

This work was supported by grants from the Department of Energy and the New York State Office of Science, Technol-

ogy, and Academic Research (NYSTAR), the Achelis-Bodman Foundation, the Lowenstein Foundation, and the New York Eye and Ear Infirmary Chairman's Research Fund.

References

1. A. Katz, E. F. Kruger, G. Minko, C. H. Liu, R. B. Rosen, and R. R. Alfano, "Detection of glutamate in the eye by Raman spectroscopy," presented at Optical Devices and Diagnostics in Materials Science, San Diego, CA (2000).
2. R. Callender, "Resonance Raman studies of visual pigments," *Annu. Rev. Biophys. Bioeng.* **6**, 33–55 (1977).
3. B. Aton, A. G. Doukas, D. Narva, R. H. Callender, U. Dinur, and B. Honig, "Resonance Raman studies of the primary photochemical event in visual pigments," *Biophys. J.* **29**, 79–94 (1980).
4. N. T. Yu, J. F. Kuck, and C. C. Askren, "Laser raman spectroscopy of the lens in situ, measured in an anesthetized rabbit," *Curr. Eye Res.* **1**, 615–618 (1981).
5. A. Mizuno, Y. Ozaki, Y. Kamada, H. Miyazaki, K. Itoh, and K. Iriyama, "Direct measurement of Raman spectra of intact lens in a whole eyeball," *Curr. Eye Res.* **1**, 609–613 (1981).
6. A. Mizuno, M. Tsuji, K. Fujii, K. Kawachi, and Y. Ozaki, "Near-infrared Fourier transform Raman spectroscopic study of cornea and sclera," *Jpn. J. Ophthalmol.* **38**, 44–48 (1994).
7. J. Sebag, S. Nie, K. Reiser, M. A. Charles, and N. T. Yu, "Raman spectroscopy of human vitreous in proliferative diabetic retinopathy," *Invest. Ophthalmol. Visual Sci.* **35**, 2976–2980 (1994).
8. I. V. Yaroslavsky, A. N. Yaroslavsky, C. Otto, G. J. Puppels, G. F. Vrensen, H. Duindam, and J. Greve, "Combined elastic and Raman light scattering of human eye lenses," *Exp. Eye Res.* **59**, 393–399 (1994).
9. D. Borchman, O. P. Lamba, Y. Ozaki, and M. Czarnecki, "Raman structural characterization of clear human lens lipid membranes," *Curr. Eye Res.* **12**, 279–284 (1993).
10. P. S. Bernstein, M. D. Yoshida, N. B. Katz, R. W. McClane, and W. Gellermann, "Raman detection of macular carotenoid pigments in intact human retina," *Invest. Ophthalmol. Visual Sci.* **39**, 2003–2011 (1998).
11. I. V. Ermakov, R. W. McClane, and W. Gellermann, "Resonant Raman detection of macular pigment levels in the living human retina," *Opt. Lett.* **26**, 202–204 (2001).
12. J. J. Baraga, M. S. Feld, and R. P. Rava, "Rapid near-infrared Raman spectroscopy of human tissue with spectrograph and CCD," *Appl. Spectrosc.* **46**, 187–190 (1992).
13. G. Zhang, S. G. Demos, and R. R. Alfano, "Far-red and NIR spectral wing emission from tissues under 532 and 632 nm photo-excitation," *Lasers Life Sci.* **9**, 1–16 (1999).
14. "Threshold limit values for chemical substances and biological exposure indices," presented at American Governmental Industrial Hygienists (1995).
15. E. B. Dreyer, D. Zurakowski, R. A. Schumer, S. M. Podos, and S. A. Lipton, "Elevated glutamate levels in the vitreous body of humans and monkeys with glaucoma," *Arch. Ophthalmol. (Chicago)* **114**, 299–305 (1996).
16. S. Vohnik, C. Hanson, R. Tuma, J. A. Fuchs, C. Woodward, and G. J. Thomas, "Conformation, stability, and active-site cysteine titrations of Escherichia coli D26A thioredoxin probed by Raman spectroscopy," *Protein Sci.* **7**, 193–200 (1998).